

SCIPP 02/38
December, 2002
hep-ph/0212136

Higgs Theory and Phenomenology in the Standard Model and MSSM

Howard E. Haber

*Santa Cruz Institute for Particle Physics,
University of California, Santa Cruz, CA 95064, U.S.A.*

Abstract

A short review of the theory and phenomenology of Higgs bosons is given, with focus on the Standard Model (SM) and the minimal supersymmetric extension of the Standard Model (MSSM). The potential for Higgs boson discovery at the Tevatron and LHC, and precision Higgs studies at the LHC and a future e^+e^- linear collider are briefly surveyed. The phenomenological challenge of the approach to the decoupling limit, where the properties of the lightest CP-even Higgs boson of the MSSM are nearly indistinguishable from those of the SM Higgs boson is emphasized.

Invited talk at
The 10th International Conference on Supersymmetry and
Unification of Fundamental Interactions (SUSY02)
17–23 June 2002, DESY Hamburg, Germany

Higgs Theory and Phenomenology in the Standard Model and MSSM

Howard E. Haber

*Santa Cruz Institute for Particle Physics
University of California, Santa Cruz, CA 95064, U.S.A.*

Abstract

A short review of the theory and phenomenology of Higgs bosons is given, with focus on the Standard Model (SM) and the minimal supersymmetric extension of the Standard Model (MSSM). The potential for Higgs boson discovery at the Tevatron and LHC, and precision Higgs studies at the LHC and a future e^+e^- linear collider are briefly surveyed. The phenomenological challenge of the approach to the decoupling limit, where the properties of the lightest CP-even Higgs boson of the MSSM are nearly indistinguishable from those of the SM Higgs boson is emphasized.

1 Introduction

Despite the great successes of the LEP, SLC and Tevatron colliders during the 1990s in verifying many detailed aspects of the Standard Model (SM), the origin of electroweak symmetry breaking has not yet been fully revealed. Nevertheless, the precision electroweak data impose some strong constraints, and seem to provide strong support for the Standard Model with a weakly-coupled Higgs boson (h_{SM}). The results of the LEP Electroweak Working Group analysis shown in fig. 1(a) yield [1]: $m_{h_{\text{SM}}} = 81^{+52}_{-33}$ GeV, and yield a 95% CL upper limit of $m_{h_{\text{SM}}} < 193$ GeV. These results reflect the logarithmic sensitivity to $m_{h_{\text{SM}}}$ via the virtual Higgs loop contributions to the various electroweak observables. The 95% CL upper limit on $m_{h_{\text{SM}}}$ is consistent with the direct searches at LEP [2] that show no conclusive evidence for the Higgs boson, and imply that $m_{h_{\text{SM}}} > 114.4$ GeV at 95% CL. Fig. 1(b) exhibits the most probable range of values for the SM Higgs mass [3]. This mass range is consistent with a weakly-coupled Higgs scalar that is expected to emerge from the scalar dynamics of a self-interacting complex Higgs doublet.

Based on the successes of the Standard Model global fits to electroweak data, one can also constrain the contributions of new physics, which can enter through W^\pm and Z boson vacuum polarization corrections. This fact has already served to rule out numerous models of strongly-coupled electroweak symmetry breaking dynamics. Nevertheless, there are some loopholes that can be exploited to circumvent the conclusion that the Standard Model with a light Higgs boson is preferred. It is possible to construct models of new physics where the goodness of the global Standard Model fit to precision electroweak data is not compromised while the strong upper limit on the Higgs mass is relaxed. In particular, one can construct effective operators [4,5] or specific models of new physics [6] where

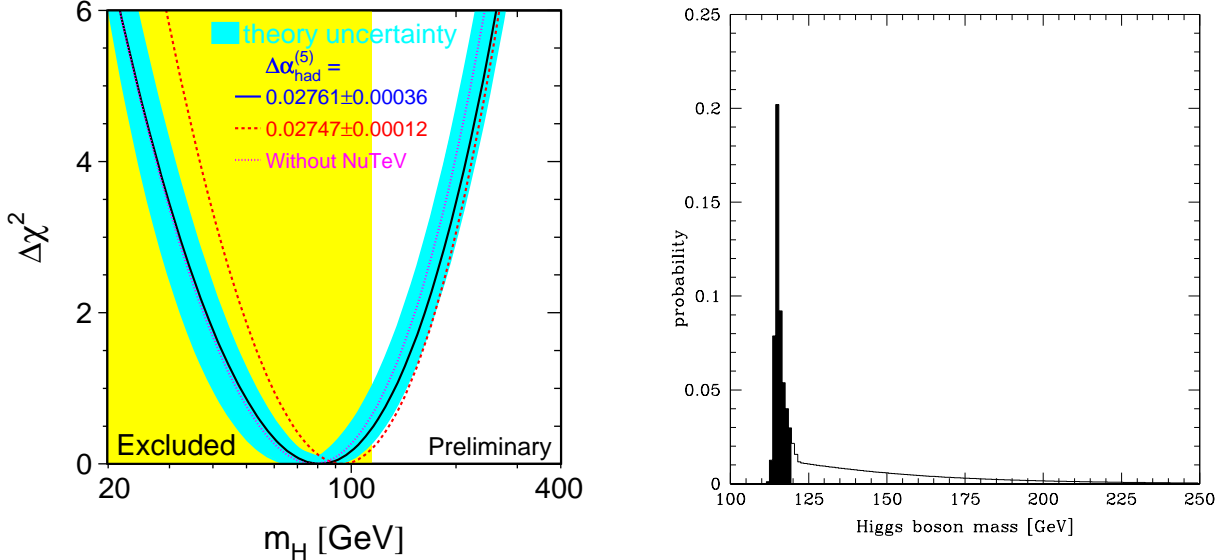


Figure 1: (a) The “blueband plot” shows $\Delta\chi^2 \equiv \chi^2 - \chi^2_{\min}$ as a function of the SM Higgs mass [1]. The solid line is a result of a global fit using all data; the band represents the theoretical error due to missing higher order corrections. The rectangular shaded region shows the 95% CL exclusion limit on the Higgs mass from direct searches at LEP [2]. (b) Probability distribution function for the Higgs boson mass, including all available direct and indirect data [3]. The probability is shown for 1 GeV bins. The shaded and unshaded regions each correspond to an integrated probability of 50%

the Higgs mass is significantly larger, but the new physics contributions to the W^\pm and Z vacuum polarizations, parameterized by the Peskin-Takeuchi [7] parameters S and T , are still consistent with the experimental data. In addition, some have argued that the global Standard Model fit exhibits some internal inconsistencies [8], which would suggest that systematic uncertainties have been underestimated and/or new physics beyond the Standard Model is required. Thus, although weakly-coupled electroweak symmetry breaking seems to be favored by the precision electroweak data, one cannot definitively rule out all other approaches. However, in this review I shall assume that the Higgs boson is indeed weakly-coupled due to electroweak symmetry breaking based on scalar dynamics.

The Standard Model is an effective field theory and provides a very good description of the physics of fundamental particles and their interactions at an energy scale of $\mathcal{O}(100)$ GeV and below. However, there must exist some energy scale, Λ , at which the Standard Model breaks down. That is, the Standard Model is no longer adequate for describing the theory above Λ , and degrees of freedom associated with new physics become relevant. Although the value of Λ is presently unknown, the Higgs mass can provide an important constraint. If $m_{h_{\text{SM}}}$ is too large, then the Higgs self-coupling blows up at some scale Λ below the Planck scale [9]. If $m_{h_{\text{SM}}}$ is too small, then the Higgs potential develops a second (global) minimum at a large value of the scalar field of order Λ [10]. Thus new physics must enter at a scale Λ or below in order that the global minimum of the theory correspond to the observed $SU(2) \times U(1)$ broken vacuum with $v = 246$ GeV.

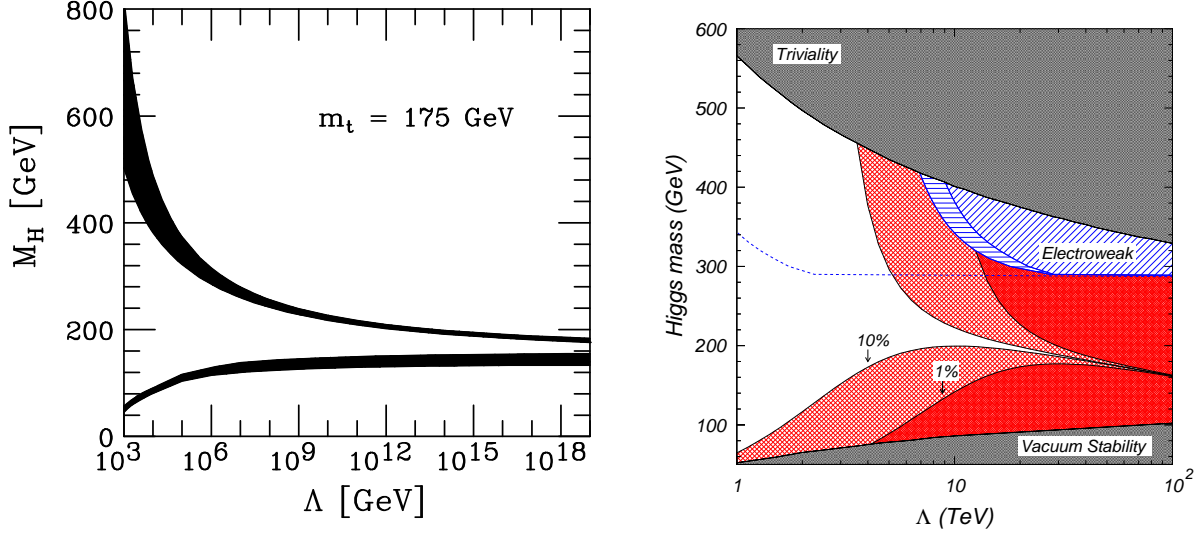


Figure 2: (a) The upper [9] and the lower [10] Higgs mass bounds as a function of the energy scale Λ at which the Standard Model breaks down, assuming $M_t = 175$ GeV and $\alpha_s(m_Z) = 0.118$, taken from ref. [11]. The shaded areas above reflect the theoretical uncertainties in the calculations of the Higgs mass bounds. (b) Following ref. [5], a reconsideration of the Λ vs. Higgs mass plot with a focus on $\Lambda < 100$ TeV. Precision electroweak measurements restrict the parameter space to lie below the dashed line, based on a 95% CL fit that allows for nonzero values of S and T and the existence of higher dimensional operators suppressed by v^2/Λ^2 . The unshaded area has less than one part in ten fine-tuning.

Given a value of Λ , one can compute the minimum and maximum Higgs mass allowed. The results of this computation (with shaded bands indicating the theoretical uncertainty of the result) are illustrated in fig. 2(a) [11]. Consequently, a Higgs mass range $130 \text{ GeV} \lesssim m_{h_{\text{SM}}} \lesssim 180 \text{ GeV}$ is consistent with an effective Standard Model that survives all the way to the Planck scale.

However, the survival of the Standard Model as an effective theory all the way up to the Planck scale is unlikely. Electroweak symmetry breaking dynamics driven by a weakly-coupled elementary scalar sector requires a mechanism for the stability of the electroweak symmetry breaking scale with respect to the Planck scale [12]. However, scalar squared-masses at one-loop order are *quadratically* sensitive to Λ . In order for this value to be consistent with the requirement that $m_{h_{\text{SM}}} \lesssim \mathcal{O}(v)$, as required from unitarity constraints [13,14], $\Lambda \lesssim 4\pi m_{h_{\text{SM}}}/g \sim \mathcal{O}(1 \text{ TeV})$ (where g is an electroweak gauge coupling). If Λ is significantly larger than 1 TeV, then the only way to generate a Higgs mass of $\mathcal{O}(v)$ is to have an “unnatural” cancellation between the bare Higgs mass and its loop corrections. The requirement of $\Lambda \sim \mathcal{O}(1 \text{ TeV})$ as a condition for the absence of fine-tuning of the Higgs mass parameter is nicely illustrated in fig. 2(b) [5].

A viable theoretical framework that incorporates weakly-coupled Higgs bosons and satisfies the naturalness constraint is that of weak-scale supersymmetry [15]. Since fermion masses are only logarithmically sensitive to Λ , boson masses will exhibit the same logarithmic sensitivity if supersymmetry is exact. However, supersymmetry is not an exact symmetry of fundamental particle interactions, and thus Λ should be identified with the energy scale of supersymmetry-breaking. Moreover, supersymmetry-breaking effects can

induce a radiative breaking of the electroweak symmetry due to the effects of the large Higgs-top quark Yukawa coupling [16]. In this way, the origin of the electroweak symmetry breaking scale is intimately tied to the mechanism of supersymmetry breaking. That is, supersymmetry provides an explanation for the stability of the hierarchy of scales, provided that supersymmetry-breaking masses in the low-energy effective electroweak theory are of $\mathcal{O}(1 \text{ TeV})$ or less [12,15]. One notable feature of the simplest weak-scale supersymmetric models is the successful unification of the electromagnetic, weak and strong gauge interactions, strongly supported by the prediction of $\sin^2 \theta_W$ at low energy scales with an accuracy at the percent level [17]. Unless one is willing to regard the apparent gauge coupling unification as a coincidence, it is tempting to conclude that electroweak symmetry breaking is indeed weakly-coupled, and new physics exists at or below a few TeV associated with the supersymmetric extension of the Standard Model.

A program of Higgs physics at future colliders must address a number of fundamental questions:

1. Does the SM Higgs boson (or a Higgs scalar with similar properties) exist?
2. How can one prove that a newly discovered scalar is a Higgs boson?
3. How many physical Higgs states are associated with the scalar sector?
4. How well can one distinguish the SM Higgs sector from a more complicated scalar sector, if only one scalar state is discovered?
5. Is the Higgs sector consistent with the constraints of supersymmetry?
6. How well can one measure the mass, width, quantum numbers and couplings strengths of the Higgs boson?
7. Are there CP-violating phenomena associated with the Higgs sector?
8. Can one reconstruct the Higgs potential and directly demonstrate the mechanism of electroweak symmetry breaking?

The physics of the Higgs bosons will be explored by experiments now underway at the upgraded proton-antiproton Tevatron collider at Fermilab and in the near future at the Large Hadron Collider (LHC) at CERN. Once evidence for the existence of new scalar particles is obtained, a more complete understanding of the scalar dynamics will require experimentation at a future e^+e^- linear collider. The next generation of high energy e^+e^- linear colliders is expected to operate at energies from 300 GeV up to about 1 TeV (JLC, NLC, TESLA), henceforth referred to as the LC [18]. With the expected high luminosities up to 1 ab^{-1} , accumulated within a few years in a clean experimental environment, these colliders are ideal instruments for reconstructing the mechanism of electroweak symmetry breaking in a comprehensive and conclusive form.

A recent comprehensive review of Higgs theory and phenomenology can be found in ref. [19], and provides an update to many topics treated in *The Higgs Hunter's Guide* [20]. In this short review, I shall highlight some of the most prominent aspects of the theory and phenomenology of Higgs bosons of the Standard Model and the MSSM.

2 The Standard Model Higgs Boson

2.1 Theory of the SM Higgs boson

In the Standard Model, the Higgs mass is given by: $m_{h_{\text{SM}}}^2 = \frac{1}{2}\lambda v^2$, where λ is the Higgs self-coupling parameter. Since λ is unknown at present, the value of the SM Higgs mass is not predicted. However, other theoretical considerations, discussed in Section 1, place constraints on the Higgs mass as exhibited in fig. 2. In contrast, the Higgs couplings to fermions [bosons] are predicted by the theory to be proportional to the corresponding particle masses [squared-masses]. In particular, the SM Higgs boson is a CP-even scalar, and its couplings to gauge bosons, Higgs bosons and fermions are given by:

$$\begin{aligned} g_{hff} &= \frac{m_f}{v}, & g_{hVV} &= \frac{2m_V^2}{v}, & g_{hhVV} &= \frac{2m_V^2}{v^2}, \\ g_{hhh} &= \frac{3}{2}\lambda v = \frac{3m_{h_{\text{SM}}}^2}{v}, & g_{hhhh} &= \frac{3}{2}\lambda = \frac{3m_{h_{\text{SM}}}^2}{v^2}, \end{aligned} \quad (1)$$

where $h \equiv h_{\text{SM}}$, $V = W$ or Z and $v = 2m_W/g = 246$ GeV. In Higgs production and decay processes, the dominant mechanisms involve the coupling of the Higgs boson to the W^\pm , Z and/or the third generation quarks and leptons. Note that a $h_{\text{SM}}gg$ coupling (g =gluon) is induced by virtue of a one-loop graph in which the Higgs boson couples to a virtual $t\bar{t}$ pair. Likewise, a $h_{\text{SM}}\gamma\gamma$ coupling is generated, although in this case the one-loop graph in which the Higgs boson couples to a virtual W^+W^- pair is the dominant contribution.

The branching ratios for the main decay modes of a SM Higgs boson are shown as a function of Higgs boson mass in fig. 3(a), based on the results obtained using the HDECAY program [21]. The total Higgs width is obtained by summing all the Higgs partial widths and is displayed as a function of Higgs mass in fig. 3(b).

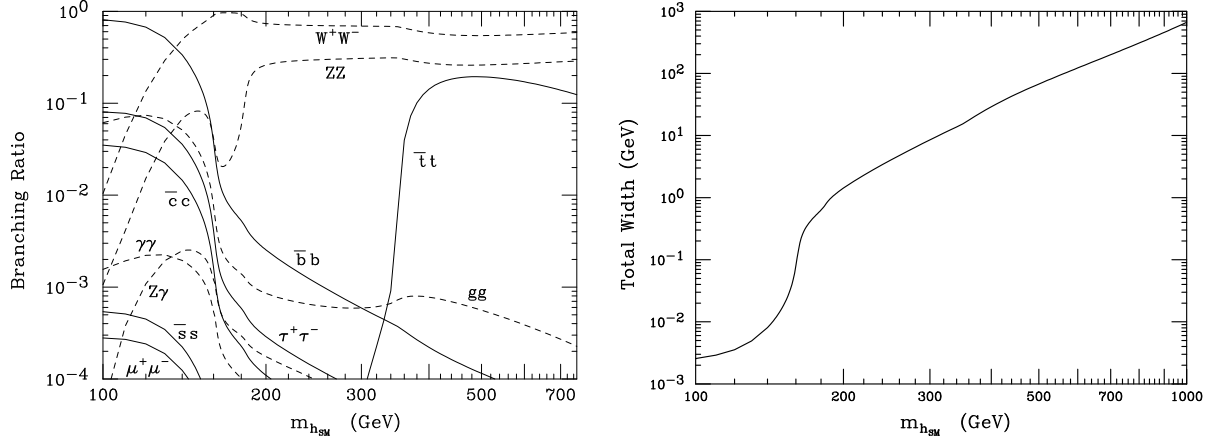


Figure 3: (a) Branching ratios of the SM Higgs boson as a function of Higgs mass. Two-boson [fermion-antifermion] final states are exhibited by solid [dashed] lines. (b) The total width of the SM Higgs boson is shown as a function of its mass.

2.2 Phenomenology of the SM Higgs boson at future colliders

The Higgs boson will be discovered first at a hadron collider. At the Tevatron, the most promising SM Higgs discovery mechanism for $m_{h_{\text{SM}}} \lesssim 135$ GeV consists of $q\bar{q}$ annihilation into a virtual V^* ($V = W$ or Z), where $V^* \rightarrow Vh_{\text{SM}}$ followed by a leptonic decay of the V and $h_{\text{SM}} \rightarrow b\bar{b}$ [22]. These processes lead to three main final states, $\ell\nu b\bar{b}$, $\nu\bar{\nu} b\bar{b}$ and $\ell^+\ell^- b\bar{b}$, that exhibit distinctive signatures on which the experiments can trigger (high p_T leptons and/or missing E_T). The backgrounds are manageable and are typically dominated by vector-boson pair production, $t\bar{t}$ production and QCD dijet production. For larger Higgs masses ($m_{h_{\text{SM}}} \gtrsim 135$ GeV) it is possible to exploit the distinct signatures present when the Higgs boson decay branching ratio to $WW^{(*)}$ becomes appreciable. In this case, there are final states with WW from the gluon-fusion production of a single Higgs boson, and WWW and ZWW arising from associated vector boson–Higgs boson production. Three search channels were identified in ref. [23] as potentially sensitive at these high Higgs masses: like-sign dilepton plus jets ($\ell^\pm\ell^\pm jj$) events, high- p_T lepton pairs plus missing E_T ($\ell^+\ell^-\nu\bar{\nu}$), and trilepton ($\ell^\pm\ell'^\pm\ell^\mp$) events. Of these, the first two were found to be most sensitive [24]. The strong angular correlations of the final state leptons resulting from WW^* is one of the crucial ingredients for these discovery channels [24,25,26].

The integrated luminosity required per Tevatron experiment, as a function of Higgs mass to either exclude the SM Higgs boson at 95% CL or discover it at the 3σ or 5σ level of significance, is shown in Fig. 4(a). These results are based on the combined statistical power of *both* the CDF and DØ experiments. The bands provide an indication of the range of uncertainty in the b -tagging efficiency, $b\bar{b}$ mass resolution and background uncertainties. It is expected that the Tevatron will reach an integrated luminosity of 2 fb^{-1} during its Run 2a phase. This will not be sufficient to extend the Higgs search much beyond the present LEP limits. There are plans to further increase the Tevatron luminosity, with a possibility of the total integrated luminosity reaching $6.5\text{--}11 \text{ fb}^{-1}$ by the end of 2008 [27]. This would provide some opportunities for the Tevatron to discover or see significant hints of Higgs boson production.

Soon after the LHC begins operation in 2007, the main Higgs search efforts will shift to CERN. A number of different Higgs production and decay channels can be studied at the LHC. The preferred channels for $m_{h_{\text{SM}}} \lesssim 200$ GeV are

$$\begin{aligned} gg &\rightarrow h_{\text{SM}} \rightarrow \gamma\gamma, \\ gg &\rightarrow h_{\text{SM}} \rightarrow VV^{(*)}, \\ qq &\rightarrow qqV^{(*)}V^{(*)} \rightarrow qqh_{\text{SM}}, \quad h_{\text{SM}} \rightarrow \gamma\gamma, \tau^+\tau^-, VV^{(*)}, \\ gg, q\bar{q} &\rightarrow t\bar{t}h_{\text{SM}}, \quad h_{\text{SM}} \rightarrow b\bar{b}, \gamma\gamma, WW^{(*)}, \end{aligned}$$

where $V = W$ or Z . The gluon-gluon fusion mechanism is the dominant Higgs production mechanism at the LHC. A recent NNLO computation of $gg \rightarrow h_{\text{SM}}$ production demonstrates the prediction for this Higgs cross-section is under theoretical control [28]. One also has appreciable Higgs production via VV electroweak gauge boson fusion, which can be separated from the gluon fusion process by employing a forward jet tag and central jet vetoing techniques. Finally, the cross-section for $t\bar{t}h_{\text{SM}}$ production [29] can be significant for $m_{h_{\text{SM}}} \lesssim 200$ GeV, although this cross-section falls faster with Higgs mass as compared to the gluon and gauge boson fusion mechanisms. Note that for $2m_W \lesssim m_{h_{\text{SM}}} \lesssim 2m_Z$,

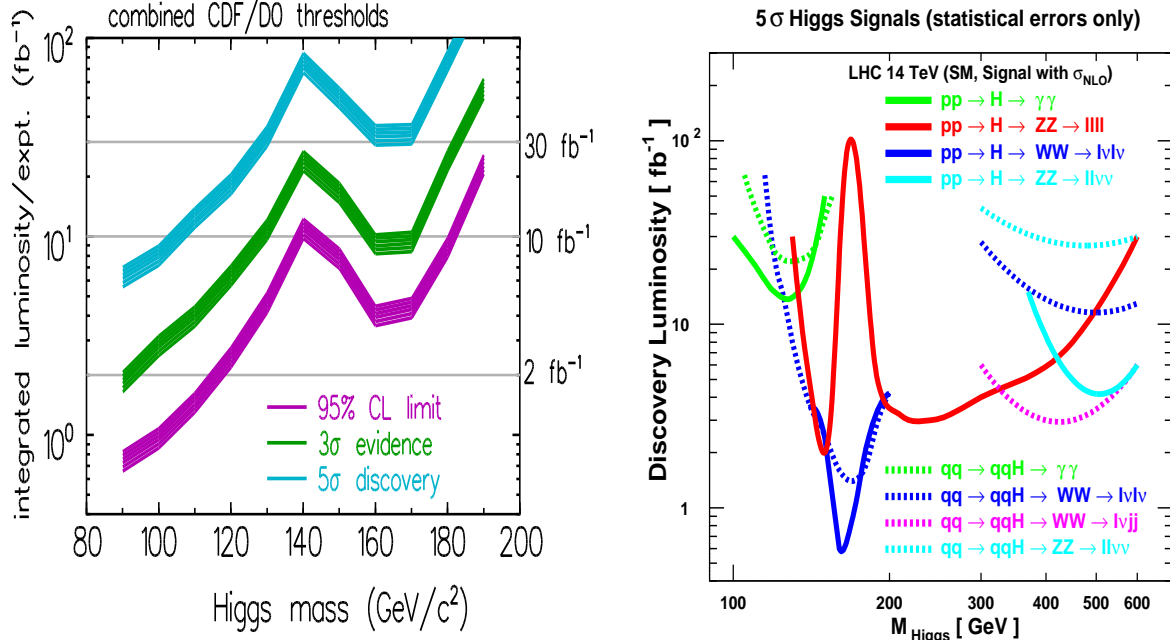


Figure 4: (a) The integrated luminosity required per Tevatron experiment, to either exclude a SM Higgs boson at 95% CL or observe it at the 3σ or 5σ level, as a function of the Higgs mass [23]. (b) Expected 5σ discovery luminosity requirements for the SM Higgs boson at the LHC for one experiment, based on a study performed with CMS fast detector simulation, assuming statistical errors only [30]. The gg and W^+W^- fusion processes are indicated respectively by the solid and dotted lines.

the Higgs branching ratio to ZZ^* is quite suppressed with respect to WW (since one of the Z bosons is off-shell). Hence, in this mass window, $h_{\text{SM}} \rightarrow W^+W^- \rightarrow \ell^+\nu\ell^-\bar{\nu}$ is the main Higgs discovery channel [26], as exhibited in fig. 4(b) [30].

The measurements of Higgs decay branching ratios at the LHC can be used to infer the values of the Higgs couplings and provide an important first step in clarifying the nature of the Higgs boson [31,32]. These can be extracted from a variety of Higgs signals that are observable over a limited range of Higgs masses. For example, for $m_{h_{\text{SM}}} \lesssim 150$ GeV, the expected accuracies of Higgs couplings to W^+W^- , $\gamma\gamma$, $\tau^+\tau^-$ and gg can be determined to an accuracy in the range of 5–15% [32]. These results are obtained under the assumption that the partial Higgs widths to W^+W^- and ZZ are fixed by electroweak gauge invariance, and the ratio of the partial Higgs widths to $b\bar{b}$ and $\tau^+\tau^-$ are fixed by the universality of Higgs couplings to down-type fermions. One can then extract the total Higgs width under the assumption that all other unobserved modes, in the Standard Model and beyond, possess small branching ratios of order 1%. The resulting accuracy anticipated is in the range of 10–25%, depending on the Higgs mass.

To significantly improve the precision of Higgs measurements, one must employ the LC [33,34,35]. The main production mechanisms of the SM Higgs boson at the LC are the Higgs-strahlung process [14,36], $e^+e^- \rightarrow Zh_{\text{SM}}$, and the WW fusion process [37] $e^+e^- \rightarrow \bar{\nu}_e\nu_e W^*W^* \rightarrow \bar{\nu}_e\nu_e h_{\text{SM}}$. With an accumulated luminosity of 500 fb⁻¹, about 10⁵ Higgs bosons can be produced by Higgs-strahlung in the theoretically preferred intermediate

mass range below 200 GeV. As \sqrt{s} is increased, the cross-section for the Higgs-strahlung process decreases as s^{-1} and is dominant at low energies, while the cross-section for the WW fusion process grows as $\ln(s/m_{h_{\text{SM}}}^2)$ and dominates at high energies. For $\sqrt{s} = 350$ and 500 GeV and an integrated luminosity of 500 fb^{-1} , this ensures the observation of the SM Higgs boson up to the production kinematical limit independently of its decay [33]. Finally, the process $e^+e^- \rightarrow t\bar{t}h_{\text{SM}}$ [38] yields a distinctive signature consisting of two W bosons and four b -quark jets, and can be observed at the LC given sufficient energy and luminosity if the Higgs mass is not too large ($m_{h_{\text{SM}}} \lesssim 200 \text{ GeV}$ at $\sqrt{s} = 800 \text{ GeV}$).

The phenomenological profile of the Higgs boson can be determined by precision measurements [31]. For example, the Higgs width can be inferred in a model-independent way, with an accuracy in the range of 5–10% (for $m_{h_{\text{SM}}} \lesssim 150 \text{ GeV}$), by combining the partial width to W^+W^- , accessible in the vector boson fusion process, with the WW^* decay branching ratio [39]. The spin and parity of the Higgs boson can be determined unambiguously from the steep onset of the excitation curve in Higgs-strahlung near the threshold and the angular correlations in this process [40]. By measuring final state angular distributions and various angular and polarization asymmetries, one can check whether the Higgs boson is a state of definite CP, or whether it exhibits CP-violating behavior in its production and/or decays [41].

Higgs decay branching ratios can be well measured for $m_{h_{\text{SM}}} \lesssim 150 \text{ GeV}$ [42,43,44,45]. When such measurements are combined with measurements of Higgs production cross-sections, the absolute values of the Higgs couplings to the W^\pm and Z gauge bosons and the Yukawa couplings to leptons and quarks can be determined to a few percent in a model-independent way. In addition, the Higgs-top quark Yukawa coupling can be inferred from the cross-section for Higgs emission off $t\bar{t}$ pairs [46]. As an example, Table 1 exhibits the anticipated fractional uncertainties in the measurements of Higgs branching ratios at the LC for $m_{h_{\text{SM}}} = 120 \text{ GeV}$. Using this data, a program **HFITTER** was developed in ref. [43]

Higgs coupling	$\delta\text{BR}/\text{BR}$	$\delta g/g$
hWW	5.1%	1.2%
hZZ	—	1.2%
htt	—	2.2%
hbb	2.4%	2.1%
hcc	8.3%	3.1%
$h\tau\tau$	5.0%	3.2%
$h\mu\mu$	$\sim 30\%$	$\sim 15\%$
hgg	5.5%	
$h\gamma\gamma$	16%	
hhh	—	$\sim 20\%$

Table 1: Expected fractional uncertainties for measurements of Higgs branching ratios $[\text{BR}(h \rightarrow X\bar{X})]$ and couplings $[g_{hXX}]$, for various choices of final state $X\bar{X}$, assuming $m_h = 120 \text{ GeV}$ at the LC. In all but four cases, the results shown are based on 500 fb^{-1} of data at $\sqrt{s} = 500 \text{ GeV}$ [43]. The results for $h\gamma\gamma$ [42], $ht\bar{t}$ [43], $h\mu\mu$ [44] and hhh [47] assume 1 ab^{-1} of data at $\sqrt{s} = 500 \text{ GeV}$ (for $\gamma\gamma$ and hh) and $\sqrt{s} = 800 \text{ GeV}$ (for $t\bar{t}$ and $\mu\mu$), respectively.

to perform a Standard Model global fit based on the measurements of the Zh_{SM} , $\nu\bar{\nu}h_{\text{SM}}$ and $t\bar{t}h_{\text{SM}}$ cross-sections and the Higgs branching ratios listed in Table 1. The output of the program is a set of Higgs couplings along with their fractional uncertainties. These results should be considered representative of what can eventually be achieved at the LC, after a more complete analysis incorporating radiative corrections has been performed.

Finally, the measurement of the Higgs self-couplings is a very ambitious task that requires the highest luminosities possible at the LC [47]. The trilinear Higgs self-coupling can be measured in double Higgs-strahlung, in which a virtual Higgs boson splits into two real Higgs particles in the final state [48]. The result of a simulation based on 1 ab^{-1} of data [47] is listed in Table 1. Such a measurement is a prerequisite for determining the form of the Higgs potential that is responsible for spontaneous electroweak symmetry breaking generated by the scalar sector dynamics.

3 Higgs Bosons of the MSSM Supersymmetry

3.1 Theory of the MSSM Higgs sector

The simplest realistic supersymmetric model of the fundamental particles is a minimal supersymmetric extension of the Standard Model (MSSM) [49], which employs the minimal particle spectrum and soft-supersymmetry-breaking terms (to parameterize the unknown fundamental mechanism of supersymmetry breaking [50]). In constructing the MSSM, both hypercharge $Y = -1$ and $Y = +1$ complex Higgs doublets are required in order to obtain an anomaly-free supersymmetric extension of the Standard Model. Thus, the MSSM contains the particle spectrum of a two-Higgs-doublet extension of the Standard Model and the corresponding supersymmetric partners.

The two-doublet Higgs sector [51] contains eight scalar degrees of freedom: one complex $Y = -1$ doublet, $\Phi_d = (\Phi_d^0, \Phi_d^-)$ and one complex $Y = +1$ doublet, $\Phi_u = (\Phi_u^+, \Phi_u^0)$. The notation reflects the form of the MSSM Higgs sector coupling to fermions: Φ_d^0 [Φ_u^0] couples exclusively to down-type [up-type] fermion pairs. When the Higgs potential is minimized, the neutral Higgs fields acquire vacuum expectation values:¹

$$\langle \Phi_d \rangle = \frac{1}{\sqrt{2}} \begin{pmatrix} v_d \\ 0 \end{pmatrix}, \quad \langle \Phi_u \rangle = \frac{1}{\sqrt{2}} \begin{pmatrix} 0 \\ v_u \end{pmatrix}, \quad (2)$$

where $\tan \beta \equiv v_u/v_d$ and the normalization has been chosen such that $v^2 \equiv v_d^2 + v_u^2 = 4m_W^2/g^2 = (246 \text{ GeV})^2$. Spontaneous electroweak symmetry breaking results in three Goldstone bosons, which are absorbed and become the longitudinal components of the W^\pm and Z . The remaining five physical Higgs particles consist of a charged Higgs pair, H^\pm , one CP-odd scalar, A and two CP-even scalars:

$$\begin{aligned} h &= -(\sqrt{2} \text{Re } \Phi_d^0 - v_d) \sin \alpha + (\sqrt{2} \text{Re } \Phi_u^0 - v_u) \cos \alpha, \\ H &= (\sqrt{2} \text{Re } \Phi_d^0 - v_d) \cos \alpha + (\sqrt{2} \text{Re } \Phi_u^0 - v_u) \sin \alpha, \end{aligned} \quad (3)$$

¹The phases of the Higgs fields can be chosen such that the vacuum expectation values are real and positive. That is, the tree-level MSSM Higgs sector conserves CP, which implies that the neutral Higgs mass eigenstates possess definite CP quantum numbers.

(with $m_h \leq m_H$). The angle α arises when the CP-even Higgs squared-mass matrix (in the $\Phi_d^0 - \Phi_u^0$ basis) is diagonalized to obtain the physical CP-even Higgs states.

The supersymmetric structure of the theory imposes constraints on the Higgs sector. For example, the Higgs self-interactions are not independent parameters; they can be expressed in terms of the electroweak gauge coupling constants. As a result, all Higgs sector parameters at tree-level are determined by two free parameters, which may be taken to be $\tan \beta$ and m_A . One significant consequence of these results is that there is a tree-level upper bound to the mass of the light CP-even Higgs boson, h . One finds that: $m_h \leq m_Z |\cos 2\beta| \leq m_Z$. This is in marked contrast to the Standard Model, in which the theory does not constrain the value of $m_{h_{\text{SM}}}$ at tree-level. The origin of this difference is easy to ascertain. In the Standard Model, $m_{h_{\text{SM}}}^2 = \frac{1}{2}\lambda v^2$ is proportional to the Higgs self-coupling λ , which is a free parameter. On the other hand, all Higgs self-coupling parameters of the MSSM are related to the squares of the electroweak gauge couplings.

In the limit of $m_A \gg m_Z$, the expressions for the Higgs masses simplify and one finds:

$$m_h^2 \simeq m_Z^2 \cos^2 2\beta, \quad m_H^2 \simeq m_A^2 + m_Z^2 \sin^2 2\beta, \quad m_{H^\pm}^2 = m_A^2 + m_W^2. \quad (4)$$

In addition, the behavior of the quantity $\cos(\beta - \alpha)$ is noteworthy in this limit. One can show that at tree level,

$$\cos^2(\beta - \alpha) = \frac{m_h^2(m_Z^2 - m_h^2)}{m_A^2(m_H^2 - m_h^2)} \simeq \frac{m_Z^4 \sin^2 4\beta}{4m_A^4}, \quad (5)$$

where the last result on the right-hand side above corresponds to the limit of large m_A . Two consequences of these results are immediately apparent. First, $m_A \simeq m_H \simeq m_{H^\pm}$, up to corrections of $\mathcal{O}(m_Z^2/m_A)$. Second, $\cos(\beta - \alpha) = 0$ up to corrections of $\mathcal{O}(m_Z^2/m_A^2)$. This limit is known as the *decoupling* limit [52] because when m_A is large, there exists an effective low-energy theory below the scale of m_A in which the effective Higgs sector consists only of one CP-even Higgs boson, h . In particular, one can check that when $\cos(\beta - \alpha) = 0$, the tree-level couplings of h are precisely those of the SM Higgs boson.

The phenomenology of the Higgs sector depends in detail on the various couplings of the Higgs bosons to gauge bosons, Higgs bosons and fermions. The couplings of the Higgs bosons to W and Z pairs typically depend on the angles α and β . The properties of the three-point and four-point Higgs boson–vector boson couplings are conveniently summarized by listing the various couplings that are proportional to either $\sin(\beta - \alpha)$ or $\cos(\beta - \alpha)$, and those couplings that are independent of α and β [20]:

$\cos(\beta - \alpha)$	$\sin(\beta - \alpha)$	angle-independent
HW^+W^-	hW^+W^-	—
HZZ	hZZ	—
ZAh	ZAH	ZH^+H^- , γH^+H^-
$W^\pm H^\mp h$	$W^\pm H^\mp H$	$W^\pm H^\mp A$
$ZW^\pm H^\mp h$	$ZW^\pm H^\mp H$	$ZW^\pm H^\mp A$
$\gamma W^\pm H^\mp h$	$\gamma W^\pm H^\mp H$	$\gamma W^\pm H^\mp A$
—	—	$VV\phi\phi$, $VVAA$, VVH^+H^-

where $\phi = h$ or H and $VV = W^+W^-$, ZZ , $Z\gamma$ or $\gamma\gamma$. Note that *all* vertices in the theory that contain at least one vector boson and *exactly one* non-minimal Higgs boson state (H , A or H^\pm) are proportional to $\cos(\beta - \alpha)$.

In the MSSM, the tree-level Higgs couplings to fermions obey the following property: Φ_d^0 couples exclusively to down-type fermion pairs and Φ_u^0 couples exclusively to up-type fermion pairs. This pattern of Higgs-fermion couplings defines the Type-II two-Higgs-doublet model [53,20]. The gauge-invariant Type-II Yukawa interactions (using 3rd family notation) are given by:

$$-\mathcal{L}_{\text{Yukawa}} = h_t [\bar{t}_R t_L \Phi_u^0 - \bar{t}_R b_L \Phi_u^+] + h_b [\bar{b}_R b_L \Phi_d^0 - \bar{b}_R t_L \Phi_d^-] + \text{h.c.}, \quad (6)$$

where $q_{R,L} \equiv \frac{1}{2}(1 \pm \gamma_5)q$. Inserting eq. (2) into eq. (6) yields a relation between the quark masses and the Yukawa couplings:

$$h_b = \frac{\sqrt{2} m_b}{v_d} = \frac{\sqrt{2} m_b}{v \cos \beta}, \quad h_t = \frac{\sqrt{2} m_t}{v_u} = \frac{\sqrt{2} m_t}{v \sin \beta}. \quad (7)$$

Similarly, one can define the Yukawa coupling of the Higgs boson to τ -leptons (the τ is a down-type fermion). The $h f \bar{f}$ couplings relative to the Standard Model value, m_f/v , are then given by

$$h b \bar{b} \quad (\text{or } h \tau^+ \tau^-) : \quad -\frac{\sin \alpha}{\cos \beta} = \sin(\beta - \alpha) - \tan \beta \cos(\beta - \alpha), \quad (8)$$

$$h t \bar{t} : \quad \frac{\cos \alpha}{\sin \beta} = \sin(\beta - \alpha) + \cot \beta \cos(\beta - \alpha). \quad (9)$$

As previously noted, $\cos(\beta - \alpha) = \mathcal{O}(m_Z^2/m_A^2)$ in the decoupling limit where $m_A \gg m_Z$. As a result, the h couplings to Standard Model particles approach values corresponding precisely to the couplings of the SM Higgs boson. There is a significant region of MSSM Higgs sector parameter space in which the decoupling limit applies, because $\cos(\beta - \alpha)$ approaches zero quite rapidly once m_A is larger than about 200 GeV. As a result, over a significant region of the MSSM parameter space, the search for the lightest CP-even Higgs boson of the MSSM is equivalent to the search for the SM Higgs boson.

The tree-level analysis of Higgs masses and couplings described above can be significantly altered once radiative corrections are included. The dominant effects arise from loops involving the third generation quarks and squarks and are proportional to the corresponding Yukawa couplings. For example, consider the tree-level upper bound on the lightest CP-even Higgs mass, $m_h \leq m_Z$, a result already ruled out by LEP data. This inequality receives quantum corrections primarily from an incomplete cancellation of top quark and top squark loops [54] (this cancellation would have been exact if supersymmetry were unbroken). Radiative corrections can also generate CP-violating effects in the Higgs sector due to CP-violating supersymmetric parameters, which enter in the loop computations [55]. Observable consequences include Higgs scalar eigenstates of mixed CP quantum numbers and CP-violating Higgs-fermion couplings. However, for simplicity, such effects are assumed to be small and are neglected in the following discussion.

The qualitative behavior of the radiative corrections can be most easily seen in the large top squark mass limit, where the splitting of the two diagonal entries and the off-diagonal entry of the top-squark squared-mass matrix are both small in comparison to

the average of the two top-squark squared-masses, $M_S^2 \equiv \frac{1}{2}(M_{t_1}^2 + M_{t_2}^2)$. In this case, the upper bound on the lightest CP-even Higgs mass is approximately given by

$$m_h^2 \lesssim m_Z^2 + \frac{3g^2 m_t^4}{8\pi^2 m_W^2} \left[\ln \left(\frac{M_S^2}{m_t^2} \right) + \frac{X_t^2}{M_S^2} \left(1 - \frac{X_t^2}{12M_S^2} \right) \right]. \quad (10)$$

More complete treatments of the radiative corrections ² show that eq. (10) somewhat overestimates the true upper bound of m_h . Nevertheless, eq. (10) correctly reflects some noteworthy features of the more precise result. First, the increase of the light CP-even Higgs mass bound beyond m_Z can be significant. This is a consequence of the m_t^4 enhancement of the one-loop radiative corrections. Second, the dependence of the light Higgs mass on the top-squark mixing parameter X_t implies that (for a given value of M_S) the upper bound of the light Higgs mass initially increases with X_t and reaches its *maximal* value for $X_t \simeq \sqrt{6}M_S$. This latter is referred to as the *maximal mixing* case (whereas $X_t = 0$ corresponds to the *minimal mixing* case). Third, note the logarithmic sensitivity to the top-squark masses. Naturalness arguments imply that the supersymmetric particle masses should not be larger than a few TeV. Still, the precise upper bound on the light Higgs mass depends on the specific choice for the upper limit of the top-squark masses.

At fixed $\tan \beta$, the maximal value of m_h is reached for $m_A \gg m_Z$. For large m_A , the maximal value of the lightest CP-even Higgs mass (m_h^{\max}) is realized at large $\tan \beta$ in the case of maximal mixing. Allowing for the uncertainty in the measured value of m_t and the uncertainty inherent in the theoretical analysis, one finds for $M_S \lesssim 2$ TeV that [56]

$$\begin{aligned} m_h^{\max} &\simeq 122 \text{ GeV}, & \text{if top-squark mixing is minimal,} \\ m_h^{\max} &\simeq 135 \text{ GeV}, & \text{if top-squark mixing is maximal.} \end{aligned} \quad (11)$$

In practice, parameters leading to maximal mixing are not expected in typical models of supersymmetry breaking. Thus, in general, the upper bound on the lightest Higgs boson mass is expected to be somewhere between the two extreme limits quoted above.

Radiative corrections can also have a significant impact on the pattern of Higgs couplings, particularly at large values of $\tan \beta$. The leading contributions to the radiatively-corrected Higgs couplings arise in two ways. First, to a good approximation the dominant Higgs propagator corrections can be absorbed into an effective (“radiatively-corrected”) mixing angle α [58]. In this approximation, $\cos(\beta - \alpha)$ is given in terms of the radiatively-corrected CP-even Higgs squared-mass matrix elements \mathcal{M}_{ij}^2 as follows

$$\cos(\beta - \alpha) = \frac{(\mathcal{M}_{11}^2 - \mathcal{M}_{22}^2) \sin 2\beta - 2\mathcal{M}_{12}^2 \cos 2\beta}{2(m_H^2 - m_h^2) \sin(\beta - \alpha)}, \quad (12)$$

Defining $\mathcal{M}^2 \equiv \mathcal{M}_0^2 + \delta\mathcal{M}^2$, where \mathcal{M}_0^2 denotes the tree-level squared-mass matrix, and noting that $\delta\mathcal{M}_{ij}^2 \sim \mathcal{O}(m_Z^2)$ and $m_H^2 - m_h^2 = m_A^2 + \mathcal{O}(m_Z^2)$, one obtains for $m_A \gg m_Z$

$$\cos(\beta - \alpha) = c \left[\frac{m_Z^2 \sin 4\beta}{2m_A^2} + \mathcal{O} \left(\frac{m_Z^4}{m_A^4} \right) \right], \quad (13)$$

²Detailed analytic approximations to the radiatively-corrected Higgs masses can be found in ref. [56]. A recent review of the status of the most complete Higgs mass computations has been given in ref. [57].

where

$$c \equiv 1 + \frac{\delta\mathcal{M}_{11}^2 - \delta\mathcal{M}_{22}^2}{2m_Z^2 \cos 2\beta} - \frac{\delta\mathcal{M}_{12}^2}{m_Z^2 \sin 2\beta}. \quad (14)$$

Using tree-level Higgs couplings with α replaced by its effective one-loop value provides a useful first approximation to the radiatively-corrected Higgs couplings.

For Higgs couplings to fermions, in addition to the radiatively-corrected value of $\cos(\beta - \alpha)$, one must also consider Yukawa vertex corrections. When these radiative corrections are included, all possible dimension-four Higgs-fermion couplings are generated. In particular, the effects of higher dimension operators can be ignored if $M_S \gg m_Z$, which we henceforth assume. These results can be summarized by an effective Lagrangian that describes the coupling of the neutral Higgs bosons to the third generation quarks:

$$-\mathcal{L}_{\text{eff}} = (h_b + \delta h_b) \bar{b}_R b_L \Phi_d^0 + (h_t + \delta h_t) \bar{t}_R t_L \Phi_u^0 + \Delta h_t \bar{t}_R t_L \Phi_d^{0*} + \Delta h_b \bar{b}_R b_L \Phi_u^{0*} + \text{h.c.}, \quad (15)$$

resulting in a modification of the tree-level relation between h_q and m_q ($q = b, t$) [59]:

$$m_b = \frac{h_b v}{\sqrt{2}} \cos \beta \left(1 + \frac{\delta h_b}{h_b} + \frac{\Delta h_b \tan \beta}{h_b} \right) \equiv \frac{h_b v}{\sqrt{2}} \cos \beta (1 + \Delta_b), \quad (16)$$

$$m_t = \frac{h_t v}{\sqrt{2}} \sin \beta \left(1 + \frac{\delta h_t}{h_t} + \frac{\Delta h_t \cot \beta}{h_t} \right) \equiv \frac{h_t v}{\sqrt{2}} \sin \beta (1 + \Delta_t). \quad (17)$$

The dominant contributions to Δ_b are $\tan \beta$ -enhanced. In particular, for $\tan \beta \gg 1$, $\Delta_b \simeq (\Delta h_b / h_b) \tan \beta$; whereas $\delta h_b / h_b$ provides a small correction to Δ_b . In the same limit, $\Delta_t \simeq \delta h_t / h_t$, with the additional contribution of $(\Delta h_t / h_t) \cot \beta$ providing a small correction. Explicitly,

$$\begin{aligned} \Delta_b &\simeq \left[\frac{2\alpha_s}{3\pi} \mu M_{\tilde{g}} I(M_{\tilde{t}_1}^2, M_{\tilde{t}_2}^2, M_{\tilde{g}}^2) + \frac{h_t^2}{16\pi^2} \mu A_t I(M_{\tilde{t}_1}^2, M_{\tilde{t}_2}^2, \mu^2) \right] \tan \beta \\ \Delta_t &\simeq -\frac{2\alpha_s}{3\pi} A_t M_{\tilde{g}} I(M_{\tilde{t}_1}^2, M_{\tilde{t}_2}^2, M_{\tilde{g}}^2) - \frac{h_b^2}{16\pi^2} \mu^2 I(M_{\tilde{b}_1}^2, M_{\tilde{b}_2}^2, \mu^2), \end{aligned}$$

where the function I is defined by:

$$I(a, b, c) = \frac{ab \ln(a/b) + bc \ln(b/c) + ca \ln(c/a)}{(a-b)(b-c)(a-c)}. \quad (18)$$

Note that I is manifestly positive and $I(a, a, a) = 1/(2a)$.

The τ couplings are obtained by replacing m_b , Δ_b and δh_b with m_τ , Δ_τ and δh_τ , respectively. At large $\tan \beta$,

$$\Delta_\tau \simeq \left[\frac{\alpha_1}{4\pi} M_1 \mu I(M_{\tilde{\tau}_1}^2, M_{\tilde{\tau}_2}^2, M_1^2) - \frac{\alpha_2}{4\pi} M_2 \mu I(M_{\tilde{\nu}_\tau}^2, M_2^2, \mu^2) \right] \tan \beta, \quad (19)$$

where $\alpha_2 \equiv g^2/4\pi$ and $\alpha_1 \equiv g'^2/4\pi$ are the electroweak gauge couplings. In general, one expects that $|\Delta_\tau| \ll |\Delta_b|$.

Including the leading radiative corrections, the $hf\bar{f}$ couplings are given by

$$\begin{aligned} h b \bar{b} : & \quad -\frac{m_b}{v} \frac{\sin \alpha}{\cos \beta} \left[1 + \frac{1}{1 + \Delta_b} \left(\frac{\delta h_b}{h_b} - \Delta_b \right) (1 + \cot \alpha \cot \beta) \right] \\ h t \bar{t} : & \quad \frac{m_t}{v} \frac{\cos \alpha}{\sin \beta} \left[1 - \frac{1}{1 + \Delta_t} \frac{\Delta h_t}{h_t} (\cot \beta + \tan \alpha) \right]. \end{aligned} \quad (20)$$

Away from the decoupling limit, the Higgs couplings to down-type fermions can deviate significantly from their tree-level values due to enhanced radiative corrections at large $\tan \beta$ [where $\Delta_b \simeq \mathcal{O}(1)$]. However, in the approach to the decoupling limit, one can work to first order in $\cos(\beta - \alpha)$ and obtain

$$\begin{aligned} g_{hbb} & \simeq g_{h_{\text{SM}}bb} \left[1 + (\tan \beta + \cot \beta) \cos(\beta - \alpha) \left(\cos^2 \beta - \frac{1 + \delta h_b/h_b}{1 + \Delta_b} \right) \right], \\ g_{htt} & \simeq g_{h_{\text{SM}}tt} \left[1 + \cos(\beta - \alpha) \left(\cot \beta - \frac{1}{1 + \Delta_t} \frac{\Delta h_t}{h_t} \frac{1}{\sin^2 \beta} \right) \right]. \end{aligned} \quad (21)$$

Note that eq. (13) implies that $(\tan \beta + \cot \beta) \cos(\beta - \alpha) \simeq \mathcal{O}(m_Z^2/m_A^2)$, even if $\tan \beta$ is very large (or small). Thus, at large m_A the deviation of the $h b \bar{b}$ coupling from its SM value vanishes as m_Z^2/m_A^2 for all values of $\tan \beta$.

Thus, if we keep only the leading $\tan \beta$ -enhanced radiative corrections, then [60]

$$\begin{aligned} \frac{g_{hVV}^2}{g_{h_{\text{SM}}VV}^2} & \simeq 1 - \frac{c^2 m_Z^4 \sin^2 4\beta}{4m_A^4}, & \frac{g_{htt}^2}{g_{h_{\text{SM}}tt}^2} & \simeq 1 + \frac{c m_Z^2 \sin 4\beta \cot \beta}{m_A^2}, \\ \frac{g_{hbb}^2}{g_{h_{\text{SM}}bb}^2} & \simeq 1 - \frac{4c m_Z^2 \cos 2\beta}{m_A^2} \left[\sin^2 \beta - \frac{\Delta_b}{1 + \Delta_b} \right]. \end{aligned} \quad (22)$$

The approach to decoupling is fastest for the h couplings to vector bosons and slowest for the couplings to down-type quarks.

Note that it is possible for h to behave like a SM Higgs boson outside the parameter regime where decoupling has set in. This phenomenon can arise if the MSSM parameters (which govern the Higgs mass radiative corrections) take values such that $c = 0$, or equivalently [from eq. (14)]:

$$2m_Z^2 \sin 2\beta = 2\delta\mathcal{M}_{12}^2 - \tan 2\beta (\delta\mathcal{M}_{11}^2 - \delta\mathcal{M}_{22}^2). \quad (23)$$

In this case, $\cos(\beta - \alpha) = 0$, due to a cancellation of the tree-level and one-loop contributions. In particular, eq. (23) is independent of the value of m_A . Typically, eq. (23) yields a solution at large $\tan \beta$. That is, by approximating $\tan 2\beta \simeq -\sin 2\beta \simeq -2/\tan \beta$, one can determine the value of $\tan \beta$ at which $\cos(\beta - \alpha) \simeq 0$ [60]:

$$\tan \beta \simeq \frac{2m_Z^2 - \delta\mathcal{M}_{11}^2 + \delta\mathcal{M}_{22}^2}{\delta\mathcal{M}_{12}^2}. \quad (24)$$

If m_A is not much larger than m_Z , then h is a SM-like Higgs boson outside the decoupling regime.

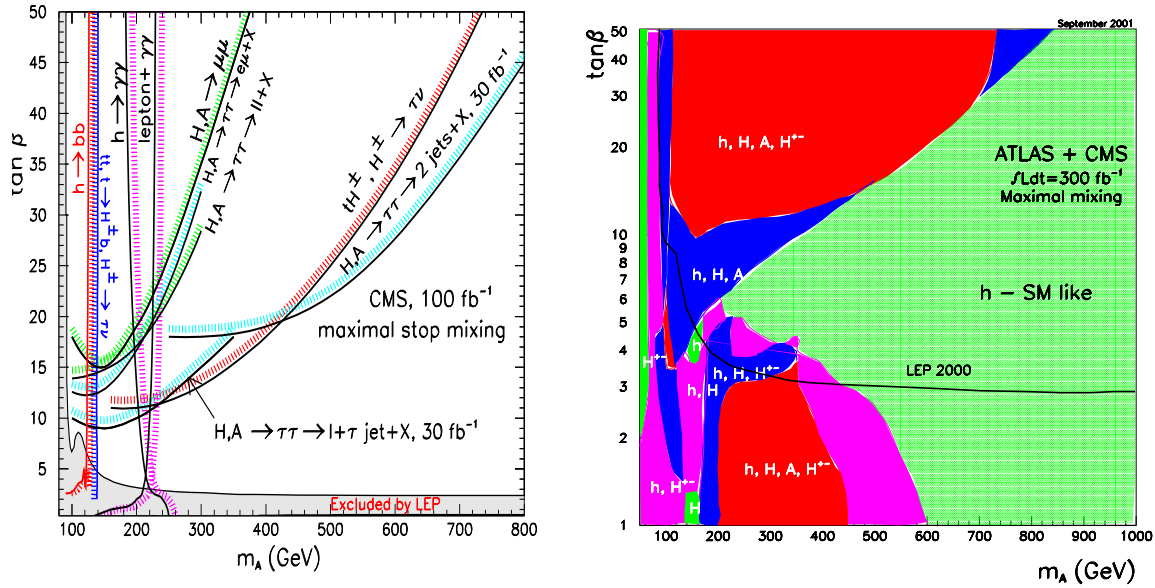


Figure 5: (a) 5σ discovery contours for MSSM Higgs boson detection in various channels in the m_A - $\tan\beta$ plane, in the maximal mixing scenario, assuming an integrated luminosity of $L = 100 \text{ fb}^{-1}$ for the CMS detector [62]. (b) Regions in the m_A - $\tan\beta$ plane in the maximal mixing scenario in which up to four Higgs boson states of the MSSM can be discovered at the LHC with 300 fb^{-1} of data, based on a simulation that combines data from the ATLAS and CMS detectors [63].

3.2 Phenomenology of MSSM Higgs bosons at future colliders

We have noted that in the decoupling regime, h of the MSSM behaves like the SM Higgs boson. Thus, for $m_A \gtrsim 200 \text{ GeV}$, the Higgs discovery reach of future colliders is nearly identical to that of the SM Higgs boson. In addition, if the heavier Higgs states are not too heavy, then they can also be directly observed. It is convenient to present the discovery contours in the m_A - $\tan\beta$ plane. At the Tevatron, there is only a small region of the parameter space in which more than one Higgs boson can be detected. This is a region of small m_A and large $\tan\beta$, where $b\bar{b}A$ production is $\tan\beta$ -enhanced [61].³

If no Higgs boson is discovered at the Tevatron, the LHC will cover the remaining unexplored regions of the m_A - $\tan\beta$ plane, as shown in fig. 5 [62,63]. That is, in the maximal mixing scenario (and probably in most regions of MSSM Higgs parameter space), at least one of the Higgs bosons is guaranteed to be discovered at the LHC. A large fraction of the parameter space can be covered in the search for a neutral CP-even Higgs boson by employing the SM Higgs search techniques, where the SM Higgs boson is replaced by h or H with the appropriate rescaling of the couplings. Moreover, fig. 5 illustrates that in some regions of the parameter space, both h and H can be simultaneously observed, and additional Higgs search techniques can be employed to discover A and/or H^{\pm} .

³In the same region of parameter space, one of the CP-even Higgs states also has an enhanced cross-section when produced in association with $b\bar{b}$. Finally, the discovery of the charged Higgs boson is possible via $t \rightarrow bH^+$ (and $\bar{t} \rightarrow \bar{b}H^-$) decay [23] if $m_{H^{\pm}} < m_t - m_b$ [since $\text{BR}(t \rightarrow bH^+)$ is non-negligible for large (and small) values of $\tan\beta$].

Thus, it may be possible at the LHC to either *exclude* the entire m_A - $\tan\beta$ plane (thereby eliminating the MSSM Higgs sector as a viable model), or achieve a 5σ discovery of at least one of the MSSM Higgs bosons, independently of the value of $\tan\beta$ and m_A . Note that over a significant fraction of the MSSM Higgs parameter space, there is still a sizable wedge-shaped region at moderate values of $\tan\beta$, opening up from about $m_A = 200$ GeV to higher values, in which the heavier Higgs bosons cannot be discovered at the LHC. In this parameter regime, only the lightest CP-even Higgs boson can be discovered, and its properties are nearly indistinguishable from those of the SM Higgs boson. Precision measurements of Higgs branching ratios and other properties will then be required in order to detect deviations from SM Higgs predictions and demonstrate the existence of a non-minimal Higgs sector.

For high precision Higgs measurements, we turn our attention to the LC. The main production mechanisms for the MSSM Higgs bosons are [64,33,35]

$$\begin{aligned}
e^+e^- &\rightarrow Zh, ZH \quad \text{via Higgs-strahlung,} \\
e^+e^- &\rightarrow \nu\bar{\nu}h, \nu\bar{\nu}H \quad \text{via } W^+W^- \text{ fusion,} \\
e^+e^- &\rightarrow hA, HA \quad \text{via } s\text{-channel } Z \text{ exchange,} \\
e^+e^- &\rightarrow H^+H^- \quad \text{via } s\text{-channel } \gamma, Z \text{ exchange.}
\end{aligned} \tag{25}$$

If $\sqrt{s} < 2m_A$, then only h production will be observable at the LC.⁴ Moreover, this region is deep within the decoupling regime, where it will be particularly challenging to distinguish h from the SM Higgs boson. As noted in Table 1, recent simulations of Higgs branching ratio measurements [43] suggest that the Higgs couplings to vector bosons and the third generation fermions can be determined with an accuracy in the range of 1–3% at the LC. In the approach to the decoupling limit, the fractional deviations of the couplings of h relative to those of h_{SM} scale as m_Z^2/m_A^2 . Thus, if precision measurements reveal a significant deviation from SM expectations, one could in principle derive a constraint (*e.g.*, upper and lower bounds) on the heavy Higgs masses.

In the MSSM, this constraint is sensitive to the supersymmetric parameters that control the radiative corrections to the Higgs couplings. This is illustrated in fig. 6, where the constraints on m_A are derived for two different sets of MSSM parameter choices [60]. Here, a simulation of a global fit of measured hbb , $h\tau\tau$ and hgg couplings is made (based on the anticipated experimental accuracies given in Table 1) and χ^2 contours are plotted indicating the constraints in the m_A - $\tan\beta$ plane, assuming that a deviation from SM Higgs boson couplings is seen. In the maximal mixing scenario shown in fig. 6(a), the constraints on m_A are significant and rather insensitive to the value of $\tan\beta$. However in some cases, as shown in fig. 6(b), a region of $\tan\beta$ may yield almost no constraint on m_A . This corresponds to the value of $\tan\beta$ given by eq. (24), and is a result of $\cos(\beta - \alpha) \simeq 0$ generated by radiative corrections [$c \simeq 0$ in eq. (13)]. Thus, one cannot extract a fully model-independent upper bound on the value of m_A beyond the kinematical limit that would be obtained if direct A production were not observed at the LC.

⁴Although hA production may still be kinematically allowed in this region, the cross-section is suppressed by a factor of $\cos^2(\beta - \alpha)$ and is hence unobservable.

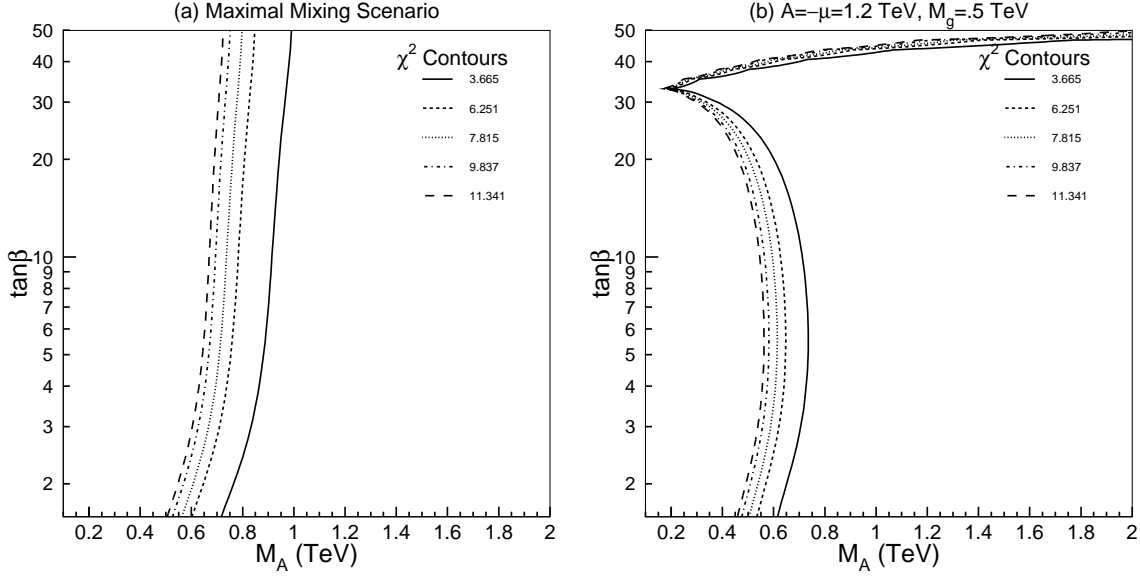


Figure 6: Contours of χ^2 for Higgs boson decay observables for (a) the maximal mixing scenario; and (b) a choice of MSSM parameters for which the loop-corrected hbb coupling is suppressed at large $\tan\beta$ and low m_A (relative to the corresponding tree-level coupling). The contours correspond to 68, 90, 95, 98 and 99% confidence levels (right to left) for the observables g_{hbb}^2 , $g_{h\tau\tau}^2$, and g_{hgg}^2 . See ref. [60] for additional details.

4 Conclusions

Precision electroweak data suggest the existence of a weakly-coupled Higgs boson. Once the Higgs boson is discovered, one must determine whether it is the SM Higgs boson, or whether there are any departures from SM Higgs predictions. Such departures will reveal crucial information about the nature of the electroweak symmetry breaking dynamics. Precision Higgs measurements are essential for detecting deviations from SM predictions of branching ratios, coupling strengths, cross-sections, *etc.* and can provide critical tests of the supersymmetric interpretation of new physics beyond the Standard Model. A program of precision Higgs measurements will begin at the LHC, but will only truly blossom at a future high energy e^+e^- linear collider.

The decoupling limit corresponds to the parameter regime in which the properties of the lightest CP-even Higgs boson are nearly indistinguishable from those of the SM Higgs boson, and all other Higgs scalars of the model are significantly heavier than the Z . Deviations from the decoupling limit may provide significant information about the non-minimal Higgs sector and can yield indirect information about the MSSM parameters. At large $\tan\beta$, there can be additional sensitivity to MSSM parameters via enhanced radiative corrections. It is possible that more than one Higgs boson is accessible to future colliders, in which case there will be many Higgs boson observables to measure and interpret. In contrast, the decoupling limit presents a severe challenge for future Higgs studies and places strong requirements on the level of precision needed to fully explore the dynamics of electroweak symmetry breaking.

Acknowledgments

Much of this work is based on a collaboration with Marcela Carena. I have greatly benefited from our many animated discussions. I am also grateful to Peter Zerwas for his kind hospitality and his contributions to our joint efforts at the Snowmass 2001 workshop. I am also pleased to acknowledge the collaboration with Jack Gunion, which contributed much to my understanding of the decoupling limit and its implications. Finally, I would like to thank Heather Logan and Steve Mrenna for many fruitful interactions.

This work is supported in part by the U.S. Department of Energy under grant no. DE-FG03-92ER40689.

References

- [1] D. Abbaneo *et al.* [LEP Electroweak Working Group] and A. Chou *et al.* [SLD Heavy Flavor and Electroweak Groups], LEPEWWG/2002-01 (8 May 2002).
- [2] ALEPH, DELPHI, L3 and OPAL Collaborations, The LEP working group for Higgs boson searches, LHWG Note 2002-01 (July 2002).
- [3] J. Erler, *Phys. Rev.* **D63** (2001) 071301.
- [4] R. Barbieri and A. Strumia, *Phys. Lett.* **B462** (1999) 144; R.S. Chivukula and N. Evans, *Phys. Lett.* **B464** (1999) 244; L.J. Hall and C. Kolda, *Phys. Lett.* **B459** (1999) 213; B.A. Kniehl and A. Sirlin, *Eur. Phys. J.* **C16** (2000) 635; J.A. Bagger, A.F. Falk and M. Swartz, *Phys. Rev. Lett.* **84** (2000) 1385.
- [5] C. Kolda and H. Murayama, *JHEP* **0007** (2000) 035.
- [6] R. Casalbuoni, S. De Curtis, D. Dominici, R. Gatto and M. Grazzini, *Phys. Lett.* **B435** (1998) 396; R.S. Chivukula, B.A. Dobrescu, H. Georgi and C.T. Hill, *Phys. Rev.* **D59** (1999) 075003; T.G. Rizzo and J.D. Wells, *Phys. Rev.* **D61** (2000) 016007; R.S. Chivukula, C. Hoelbling and N. Evans, *Phys. Rev. Lett.* **85** (2000) 511; P. Chankowski, T. Farris, B. Grzadkowski, J.F. Gunion, J. Kalinowski and M. Krawczyk, *Phys. Lett.* **B496** (2000) 195; H.C. Cheng, B.A. Dobrescu and C.T. Hill, *Nucl. Phys.* **B589** (2000) 249; H.J. He, N. Polonsky and S.F. Su, *Phys. Rev.* **D64** (2001) 053004; M.E. Peskin and J.D. Wells, *Phys. Rev.* **D64** (2001) 093003; H.J. He, C.T. Hill and T.M. Tait, *Phys. Rev.* **D65** (2002) 055006.
- [7] M.E. Peskin and T. Takeuchi, *Phys. Rev. Lett.* **65** (1990) 964, *Phys. Rev.* **D46** (1992) 381.
- [8] G. Altarelli, F. Caravaglios, G.F. Giudice, P. Gambino and G. Ridolfi, *JHEP* **0106** (2001) 018; M.S. Chanowitz, *Phys. Rev. Lett.* **87** (2001) 231802; *Phys. Rev.* **D66** (2002) 073002; D. Choudhury, T.M. Tait and C.E.M. Wagner, *Phys. Rev.* **D65** (2002) 053002; S. Davidson, S. Forte, P. Gambino, N. Rius and A. Strumia, *JHEP* **0202** (2002) 037; W. Loinaz, N. Okamura, T. Takeuchi and L.C. Wijewardhana, hep-ph/0210193.

- [9] T. Hambye and K. Riesselmann, *Phys. Rev.* **D55** (1997) 7255.
- [10] See, *e.g.*, G. Altarelli and G. Isidori, *Phys. Lett.* **B337** (1994) 141; J.A. Casas, J.R. Espinosa and M. Quirós, *Phys. Lett.* **B342** (1995) 171; **B382** (1996) 374.
- [11] K. Riesselmann, DESY-97-222 (1997) [hep-ph/9711456].
- [12] For a review, see L. Susskind, *Phys. Reports* **104** (1984) 181.
- [13] J.M. Cornwall, D.N. Levin and G. Tiktopoulos, *Phys. Rev. Lett.* **30** (1973) 1268; *Phys. Rev.* **D10** (1974) 1145; C.H. Llewellyn Smith, *Phys. Lett.* **46B** (1973) 233.
- [14] B.W. Lee, C. Quigg and H.B. Thacker, *Phys. Rev.* **D16** (1977) 1519.
- [15] E. Witten, *Nucl. Phys.* **B188** (1981) 513; S. Dimopoulos and H. Georgi, *Nucl. Phys.* **B193** (1981) 150; R.K. Kaul, *Phys. Lett.* **109B**, 19 (1982); *Pramana* **19**, 183 (1982).
- [16] L.E. Ibáñez and G.G. Ross, *Phys. Lett.* **B110** (1982) 215; L.E. Ibáñez, *Phys. Lett.* **B118** (1982) 73; J. Ellis, D.V. Nanopoulos and K. Tamvakis, *Phys. Lett.* **B121** (1983) 123; L. Alvarez-Gaumé, J. Polchinski and M.B. Wise, *Nucl. Phys.* **B221** (1983) 495.
- [17] For a review, see S. Raby in the *2002 Review of Particle Physics*, K. Hagiwara *et al.* [Particle Data Group], *Phys. Rev.* **D66** (2002) 010001.
- [18] N. Akasaka *et al.*, “JLC design study,” KEK-REPORT-97-1; C. Adolphsen *et al.* [International Study Group Collaboration], “International study group progress report on linear collider development,” SLAC-R-559 and KEK-REPORT-2000-7 (April, 2000); R. Brinkmann, K. Flottmann, J. Rossbach, P. Schmuser, N. Walker and H. Weise [editors], “TESLA: The superconducting electron positron linear collider with an integrated X-ray laser laboratory. Technical design report, Part 2: The Accelerator,” DESY-01-011 (March, 2001) [<http://tesla.desy.de/tdr/>].
- [19] M. Carena and H.E. Haber, FERMILAB-Pub-02/114-T [hep-ph/0208209].
- [20] J.F. Gunion, H.E. Haber, G. Kane and S. Dawson, *The Higgs Hunter’s Guide* (Perseus Publishing, Cambridge, MA, 1990).
- [21] A. Djouadi, J. Kalinowski and M. Spira, *Comp. Phys. Commun.* **108** (1998) 56. HDECAY is available from <http://home.cern.ch/~mspira/proglist.html>.
- [22] A. Stange, W. Marciano and S. Willenbrock, *Phys. Rev.* **D49** (1994) 1354; **D50** (1994) 4491.
- [23] M. Carena, J.S. Conway, H.E. Haber, J. Hobbs *et al.*, Report of the Tevatron Higgs Working Group, hep-ph/0010338.
- [24] T. Han, A.S. Turcot and R.-J. Zhang, *Phys. Rev.* **D59** (1999) 093001.
- [25] C. Nelson, *Phys. Rev.* **D37** (1988) 1220.
- [26] M. Dittmar and H. Dreiner, *Phys. Rev.* **D55** (1997) 167.

- [27] M. Witherell, “The Fermilab Program and the FY2003 Budget,” presented at HEPAP meeting, 7 November, 2002.
- [28] R.V. Harlander and W.B. Kilgore, *Phys. Rev. Lett.* **88** (2002) 201801; C. Anastasiou and K. Melnikov, *Nucl. Phys.* **B646** (2002) 220.
- [29] W. Beenakker, S. Dittmaier, M. Kramer, B. Plumper, M. Spira and P.M. Zerwas, *Phys. Rev. Lett.* **87** (2001) 201805. L. Reina and S. Dawson, *Phys. Rev. Lett.* **87** (2001) 201804; L. Reina, S. Dawson and D. Wackeroth, *Phys. Rev.* **D65** (2002) 053017; S. Dawson, L.H. Orr, L. Reina and D. Wackeroth, hep-ph/0211438.
- [30] M. Dittmar, *Pramana* **55** (2000) 151; M. Dittmar and A.-S. Nicollerat, “High Mass Higgs Studies using $gg \rightarrow h_{\text{SM}}$ and $qq \rightarrow qqh_{\text{SM}}$ at the LHC,” CMS-NOTE 2001/036.
- [31] J.F. Gunion, L. Poggioli, R. Van Kooten, C. Kao and P. Rowson, in *New Directions for High Energy Physics*, Proceedings of the 1996 DPF/DPB Summer Study on High Energy Physics, Snowmass ’96, edited by D.G. Cassel, L.T. Gennari and R.H. Siemann (Stanford Linear Accelerator Center, Stanford, CA, 1997) pp. 541–587.
- [32] D. Zeppenfeld, R. Kinnunen, A. Nikitenko and E. Richter-Was, *Phys. Rev.* **D62** (2000) 013009; T. Plehn, D. Rainwater and D. Zeppenfeld, *Phys. Rev. Lett.* **88** (2002) 051801.
- [33] R.D. Heuer, D.J. Miller, F. Richard and P.M. Zerwas [editors], “TESLA: The superconducting electron positron linear collider with an integrated X-ray laser laboratory. Technical design report, Part 3: Physics at an e^+e^- Linear Collider,” DESY-01-011 (March, 2001), <http://tesla.desy.de/tdr/> [hep-ph/0106315].
- [34] M. Battaglia, hep-ph/0211461, in these Proceedings.
- [35] J.F. Gunion, H.E. Haber and R. Van Kooten, “Higgs Physics at the Linear Collider,” to appear in *Linear Collider Physics in the New Millennium*, edited by K. Fujii, D. Miller and A. Soni.
- [36] J. Ellis, M.K. Gaillard, D.V. Nanopoulos, *Nucl. Phys.* **B106** (1976) 292; B.L. Ioffe, V.A. Khoze. *Sov. J. Nucl. Phys.* **9** (1978) 50.
- [37] D.R.T. Jones and S. Petcov, *Phys. Lett.* **B84** (1979) 440; R.N. Cahn and S. Dawson, *Phys. Lett.* **B136** (1984) 196; G.L. Kane, W.W. Repko and W.B. Rolnick, *Phys. Lett.* **B148** (1984) 367; G. Altarelli, B. Mele and F. Pitolli, *Nucl. Phys.* **B287** (1987) 205; W. Kilian, M. Krämer and P.M. Zerwas, *Phys. Lett.* **B373** (1996) 135.
- [38] K.J. Gaemers and G.J. Gounaris, *Phys. Lett.* **77B** (1978) 379; A. Djouadi, J. Kalinowski and P. M. Zerwas, *Z. Phys.* **C54** (1992) 255; B.A. Kniehl, F. Madricardo and M. Steinhauser, *Phys. Rev.* **D66** (2002) 054016.
- [39] K. Desch and N. Meyer, LC Note LC-PHSM-2001-025.
- [40] V.D. Barger, K. Cheung, A. Djouadi, B.A. Kniehl and P.M. Zerwas, *Phys. Rev.* **D49** (1994) 79.

- [41] D. Chang, W.-Y. Keung and I. Phillips, *Phys. Rev.* **D48** (1993) 3225; A. Soni and R.M. Xu, *Phys. Rev.* **D48** (1993) 5259; A. Skjold and P. Osland, *Phys. Lett.* **B329** (1994) 305; *Nucl. Phys.* **B453** (1995) 3; B. Grzadkowski and J.F. Gunion, *Phys. Lett.* **B350** (1995) 218; T. Han and J. Jiang, *Phys. Rev.* **D63** (2001) 096007.
- [42] E. Boos, J.C. Brient, D.W. Reid, H.J. Schreiber and R. Shanidze, *Eur. Phys. J.* **C19** (2001) 455.
- [43] K. Desch and M. Battaglia, in *Physics and experiments with future linear e^+e^- colliders*, Proceedings of the 5th International Linear Collider Workshop, Batavia, IL, USA, 2000, edited by A. Para and H.E. Fisk (American Institute of Physics, New York, 2001), pp. 312–316; M. Battaglia and K. Desch, in *ibid.*, pp. 163–182.
- [44] M. Battaglia and A. De Roeck, in *Proceedings of the APS/DPF/DPB Summer Study on the Future of Particle Physics* (Snowmass 2001), edited by R. Davidson and C. Quigg SNOWMASS-2001-E3066 [hep-ph/0111307].
- [45] C.T. Potter, J.E. Brau and M. Iwasaki, in *Proceedings of the APS/DPF/DPB Summer Study on the Future of Particle Physics* (Snowmass 2001), edited by R. Davidson and C. Quigg, SNOWMASS-2001-P118.
- [46] J.F. Gunion, B. Grzadkowski and X.G. He, *Phys. Rev. Lett.* **77** (1996) 5172; S. Dittmaier, M. Kramer, Y. Liao, M. Spira and P.M. Zerwas, *Phys. Lett.* **B441** (1998) 383; **B478** (2000) 247; S. Dawson and L. Reina, *Phys. Rev.* **D59** (1999) 054012; H. Baer, S. Dawson and L. Reina, *Phys. Rev.* **D61** (2000) 013002; A. Juste and G. Merino, hep-ph/9910301.
- [47] M. Battaglia, E. Boos and W. Yao, in *Proceedings of the APS/DPF/DPB Summer Study on the Future of Particle Physics* (Snowmass 2001), edited by R. Davidson and C. Quigg, SNOWMASS-2001-E3016 [hep-ph/0111276].
- [48] A. Djouadi, H.E. Haber and P.M. Zerwas, *Phys. Lett.* **B375** (1996) 203; F. Boudjema and E. Chopin, *Z. Phys.* **C73** (1996) 85; D.J. Miller and S. Moretti, *Eur. Phys. J.* **C13** (2000) 459; A. Djouadi, W. Kilian, M. Mühlleitner and P.M. Zerwas, *Eur. Phys. J.* **C10** (1999) 27; C. Castanier, P. Gay, P. Lutz and J. Orloff, LC Note LC-PHSM-2000-061 [hep-ex/0101028].
- [49] H.P. Nilles, *Phys. Reports* **110** (1984) 1; H.E. Haber and G.L. Kane, *Phys. Reports* **117** (1985) 75; S.P. Martin, hep-ph/9709356.
- [50] L. Girardello and M.T. Grisaru, *Nucl. Phys.* **B194** (1982) 65; A. Pomarol and S. Dimopoulos, *Nucl. Phys.* **B453** (1995) 83.
- [51] K. Inoue, A. Kakuto, H. Komatsu, and S. Takeshita, *Prog. Theor. Phys.* **67** (1982) 1889; R. Flores and M. Sher, *Annals Phys.* **148** (1983) 95; J.F. Gunion and H.E. Haber, *Nucl. Phys.* **B272** (1986) 1 [E: **B402** (1993) 567].
- [52] H.E. Haber and Y. Nir, *Phys. Lett.* **B306** (1993) 327; J.F. Gunion and H.E. Haber, SCIPP-02/10 and UCD-2002-10 [hep-ph/0207010].

- [53] L.J. Hall and M.B. Wise, *Nucl. Phys.* **B187** (1981) 397.
- [54] H.E. Haber and R. Hempfling, *Phys. Rev. Lett.* **66** (1991) 1815; Y. Okada, M. Yamaguchi and T. Yanagida, *Prog. Theor. Phys.* **85** (1991) 1; J.R. Ellis, G. Ridolfi and F. Zwirner, *Phys. Lett.* **B257** (1991) 83.
- [55] A. Pilaftsis, *Phys. Lett.* **B435** (1998) 88; K.S. Babu, C.F. Kolda, J. March-Russell and F. Wilczek, *Phys. Rev.* **D59** (1999) 016004; D.A. Demir, *Phys. Rev.* **D60** (1999) 055006; S.Y. Choi, M. Drees and J.S. Lee, *Phys. Lett.* **B481** (2000) 57; M. Carena, J. Ellis, A. Pilaftsis and C.E.M. Wagner, *Phys. Lett.* **B495** (2000) 155; M. Carena, J.R. Ellis, A. Pilaftsis, C.E.M. Wagner, *Nucl. Phys.* **B586** (2000) 92; *Nucl. Phys.* **B625** (2002) 345; S. Heinemeyer, *Eur. Phys. J.* **C22** (2001) 521.
- [56] M. Carena, J.R. Espinosa, M. Quirós and C.E.M. Wagner, *Phys. Lett.* **B355** (1995) 209; M. Carena, M. Quirós and C.E.M. Wagner, *Nucl. Phys.* **B461** (1996) 407; H.E. Haber, R. Hempfling and A.H. Hoang, *Z. Phys.* **C75** (1997) 539; S. Heinemeyer, W. Hollik and G. Weiglein, *Phys. Lett.* **B455** (1999) 179; M. Carena, H.E. Haber, S. Heinemeyer, W. Hollik, C.E.M. Wagner and G. Weiglein, *Nucl. Phys.* **B580** (2000) 29; J.R. Espinosa and R. J. Zhang, *Nucl. Phys.* **B586** (2000) 3; J.R. Espinosa and I. Navarro, *Nucl. Phys.* **B615** (2001) 82; A. Brignole, G. Degrossi, P. Slavich and F. Zwirner, *Nucl. Phys.* **B631** (2002) 195; **B643** (2002) 79.
- [57] G. Degrossi, S. Heinemeyer, W. Hollik, P. Slavich and G. Weiglein, hep-ph/0212020.
- [58] S. Heinemeyer, W. Hollik and G. Weiglein, *Eur. Phys. J.* **C16** (2000) 139.
- [59] R. Hempfling, *Phys. Rev.* **D49** (1994) 6168; L. Hall, R. Rattazzi and U. Sarid, *Phys. Rev.* **D50** (1994) 7048; M. Carena, M. Olechowski, S. Pokorski and C.E.M. Wagner, *Nucl. Phys.* **B426** (1994) 269; J.A. Coarasa, R.A. Jiménez and J. Solà, *Phys. Lett.* **B389** (1996) 312; R.A. Jiménez and J. Solà, *Phys. Lett.* **B389** (1996) 53; A. Bartl, H. Eberl, K. Hikasa, T. Kon, W. Majerotto and Y. Yamada, *Phys. Lett.* **B378** (1996) 167; D.M. Pierce, J.A. Bagger, K. Matchev, and R. Zhang, *Nucl. Phys.* **B491** (1997) 3.
- [60] M. Carena, H.E. Haber, H.E. Logan and S. Mrenna, *Phys. Rev.* **D65** (2002) 055005 [E: **D65** (2002) 099902].
- [61] J. Dai, J.F. Gunion and R. Vega, *Phys. Lett.* **B371** (1996) 71; **B387** (1996) 801; J.L. Diaz-Cruz, H.J. He, T. Tait and C.P. Yuan, *Phys. Rev. Lett.* **80** (1998) 4641; C. Balázs, J.L. Diaz-Cruz, H.-J. He, T. Tait and C.P. Yuan, *Phys. Rev.* **D59** (1999) 055016.
- [62] D. Denegri *et al.*, CMS NOTE 2001/032 [hep-ph/0112045].
- [63] F. Gianotti, M.L. Mangano and T. Virdee conveners, *Physics Potential and Experimental Challenges of the LHC Luminosity Upgrade*, hep-ph/0204087.
- [64] J.F. Gunion, L. Roszkowski, A. Turski, H.E. Haber, G. Gamberini, B. Kayser, S.F. Novaes, F.I. Olness and J. Wudka, *Phys. Rev.* **D38** (1988) 3444.